Hindawi
Journal of Mathematics
Volume 2022, Article ID 7407924, 16 pages
https://doi.org/10.1155/2022/7407924

Research Article

Studies of Metal Organic Networks via M-Polynomial-Based Topological Indices

Muhammad Tanveer Hussain,[1] Muhammad Javaid,[1] Sajida Parveen,[1] Hafiz Muhammad Awais,[1] and Md Nur Alam[2]

[1]*Department of Mathematics, School of Science, University of Management and Technology, Lahore, Pakistan*
[2]*Department of Mathematics, Pabna University of Science and Technology, Pabna 6600, Bangladesh*

Correspondence should be addressed to Md Nur Alam; nuralam23@pust.ac.bd

Received 9 February 2022; Accepted 9 March 2022; Published 12 May 2022

Academic Editor: Gohar Ali

Topological index (TI) is a graph-theoretic tool that is used to study different physical and structural properties of the networks in various disciplines of science such as computer science, chemistry, and information technology. In this article, we study transition metal tetra-cyano-benzene organic networks by computing their M-polynomials and various topological indices (TIs). At the end, a comparison is also included between all the computed degree-based topological indices to show their betterness.

1. Introduction

Metal-organic networks (MONs) is a modern class of porous materials constructed with organic linkers based on secondary building units and metal clusters, with significant attention in the last years. Consequently, their structural diversity, high-grade porosity, and compositional tenability represent the exciting of the various physicochemical characteristics such as the grafting active group [1], postsynthetic ligand, changing organic ligand [2], preparing composites with various substances [3, 4], ions exchange [5], and impregnating suitable active materials [6], methane, and hydrogen storage materials that involve magnesium-decorated fullerenes within metal-organic frameworks [7, 8]. Seetharaj et al. [9] studied the relationship among different solvents, architecture, temperature, molar ratio, and pH of the MONs. Therefore, MONs are also studied for the purification and separation of various liquids and gases, energy storage tools in batteries [10], and precursor for the formation of nanostructures [11–13] and later on, the idea of composition of linkers with the assistance of MONs for topological insight [14–16].

Graph theory presents the modern tools which are used to study the chemical compounds and to discuss their properties. The calculated TIs of the molecular graphs are the numeric values that describe chemical reactivity, biological activity, and physical property of chemical compounds such as heat of evaporation and formation; melting, boiling and flash points, surface tension, retention time in chromatography, pressure, temperature, density, and partition coefficients [17]. Bruckler et al. [18] considered Q-indices that consist of contributions of vertex pairs that exponentially decrease with distance; Gonzalez-Diaz et al. [19] reviewed and commented on the "quo vadis" and challenges in the definition of TIs as we enter the new century; Klavzar and Gutman [20] used the bound $4W < \mathrm{MTI} < 6.93W$ that implies that W and MTI are linearly correlated not only in the case of acyclic molecules but also in the case of molecules with arbitrarily many cycles; Matamala and Estrada [21] provided the role of topological structure in the study of molecular physicochemical properties; Randic [22] reported that the sensitivity of TIs for structural changes within comprehensive groups of cyclic saturated hydrocarbons is evaluated. For more details, see [23–25].

Moreover, Wiener defined a distance-based topological index in graph theory for the boiling point of paraffin [26]. Gutman and Trinajstic [27] defined TIs named as 1st and 2nd Zagreb indices to compute the total π-electrons energy of different organic molecules [27]. TIs represent a valuable role in the quantitative structure-activity/property relationships to characterize a graph (network) with a biological and chemical property or activity. This mathematical relationship is represented as $\mathbf{P} = \mathbf{f}(\mathbf{M})$, where $\mathbf{P}$ is an activity or property and $\mathbf{M}$ is any network [28, 29]. Therefore, TIs of many networks such as silicate, honeycomb, and hexagonal networks [30], rhombous silicate and rhombus oxide networks [31], titania nanotube [32], superconducting materials [33], MOFs [34], hexagonal parallelogram nanotube [35], fullerene networks and carbon nanotube [36], regular hexagonal lattice [37], graphs with given number of cut vertices [38], and explore trees in terms of given number of vertices of maximum degree [39] are studied in the literature.

In this article, we solve the new M-polynomials, and by using these M-polynomials, the different TIs are calculated for the metal-organic networks. In the end, some comparisons between the computed TIs with the help of graphs are also included. The remaining portion is arranged as follows: Section 2 contains various definitions as well as techniques that are used in calculated results. Sections 3 and 4 present the main results of M-polynomials which are utilized in topological indices. Section 5 involves the numerical and graphical demonstration and final remarks.

2. Preliminaries

A network $\mathscr{G} = (V(\mathscr{G}), E(\mathscr{G}))$, where $V(\mathscr{G}) = \{x_1, x_2, x_3, \ldots, x_n\}$ and $E(\mathscr{G}) \subseteq V(\mathscr{G}) \times V(\mathscr{G})$ are the organic ligands (metal node) and bonds between the nodes of $\mathscr{G}$, respectively. $|V(\mathscr{G})| = v$ and $|E(\mathscr{G})| = e$ are defined as the order and size of a graph $\mathscr{G}$. In connected and simple graphs, a path is occurring between two atoms (vertices) and the distance between two atoms x and y is the length of the shortest path that is shown as $\varphi(x, y)$, in $\mathscr{G}$ [22, 40].

1st and 2nd Zagreb indices: let $\mathscr{G}$ be a simple graph; then, its 1st and 2nd Zagreb indices are

$$M_1(\mathscr{G}) = \sum_{x\in V(\mathscr{G})} [\varphi(x)]^2 = \sum_{xy\in E(\mathscr{G})} [\varphi(x) + \varphi(y)],$$
$$M_2(\mathscr{G}) = \sum_{xy\in E(\mathscr{G})} [\varphi(x) \times \varphi(y)]. \tag{1}$$

General Randic index: for a graph $\mathscr{G}$, set of real number R, and $\beta \in R$, the general Randi c' index is

$$R_\beta(\mathscr{G}) = \sum_{xy\in E(\mathscr{G})} [\varphi(x)\varphi(y)]^\beta. \tag{2}$$

Symmetric division deg index: let $\mathscr{G}$ be a simple and connected graph; then, the symmetric division deg index is

$$\mathrm{SDD}(\mathscr{G}) = \sum_{xy\in E(\mathscr{G})} \left[\frac{\min(\varphi(x), \varphi(y))}{\max(\varphi(x), \varphi(y))}\right] + \left[\frac{\max(\varphi(x), \varphi(y))}{\min(\varphi(x), \varphi(y))}\right]. \tag{3}$$

Harmonic index: let $\mathscr{G}$ be a simple graph; then, its harmonic index is

$$H(\mathscr{G}) = \sum_{xy\in E(\mathscr{G})} \frac{2}{\varphi(x) + \varphi(y)}. \tag{4}$$

Inverse sum index: let $\mathscr{G}$ be a simple graph; the inverse sum index is

$$\mathrm{IS}(\mathscr{G}) = \sum_{xy\in E(\mathscr{G})} \frac{\varphi(x)\varphi(y)}{\varphi(x) + \varphi(y)}. \tag{5}$$

Augmented Zagreb index: let $\mathscr{G}$ be a simple graph; then, the augmented Zagreb index is

$$\mathrm{AZI}(\mathscr{G}) = \sum_{xy\in E(\mathscr{G})} \left[\frac{\varphi(x) \times \varphi(y)}{\varphi(x) + \varphi(y) - 2}\right]^3. \tag{6}$$

M-polynomial: for a graph $\mathscr{G}$ and $m_{s,t}(\mathscr{G}), s, t \geq 1$ be the number of bonds (edges) $e = xy$ of $\mathscr{G}$ in such a way $\{\varphi(x)\varphi(y)\} = \{g, h\}$. Then, M-polynomial of $\mathscr{G}$ is

$$M(\mathscr{G}, g, h) = \sum_{s\leq t} m_{s,t}(\mathscr{G}) g^s h^t. \tag{7}$$

In Tables 1 and 2, the relationship among the aforesaid TIs and the M-polynomial is given.

Moreover, $D_g = \phi(f(g,h))/\phi(g)$, $D_h = \phi(f(g,h))/\phi(h)$, $S_g = \int_0^g (\phi(f(t,h))/t)\mathrm{d}t$, $S_h = \int_0^h (\phi(f(g,t))/t)\mathrm{d}t$, $J(f(g,h)) = (f(g,g))$, and $Q_\beta(f(g,h)) = g_\beta(f(g,h))$, where $\beta \neq 0$. For further detailed discussion, refer to [41]. Metal-organic networks are considered such types of networks that are investigated for constant porosity. Therefore, these porous materials are filled with gas or liquid. Such types of pores are made with the help of metal nodes and organic ligands. The organic molecules are organic ligands that might be held together to form coordination. In organic chemistry, ligands are recognized as molecules or ions that are related to different types of functional groups attached to a central atom to form complicated coordination, i.e., coordinate covalent bonds between the central atom and ligands. These networks with porosity form in such a way that ligands attached in different places and metals place only in the middle of the network. Moreover, MONs are considered to be in two or three-dimensional networks. In the current discussion, we are dealing with MON, TM-TCNB (TM, transition metals of the 3rd series: titanium, vanadium, chromium, and zinc, where transition metals (group B elements) occupy the middle section (d-block) of the periodic table; TCNB, tetra-cyano-benzene). The two-dimensional

Table 1: Derivation of TIs from M-polynomial.

Indices	$f(g,h)$	Derivation from $M(\mathscr{G},g,h)$
M_1	$g+h$	$(D_g+D_h)(M(\mathscr{G},g,h))\|_{g=1=h}$
M_2	gh	$(D_gD_h)(M(\mathscr{G},g,h))\|_{g=1=h}$
MM_2	$1/gh$	$(S_gS_h)(M(\mathscr{G},g,h))\|_{g=1=h}$
R_β	$(gh)^\beta, \beta\in N$	$(D_g^\beta D_h^\beta)(M(\mathscr{G},g,h))\|_{g=1=h}$
$R_\beta R_\beta$	$(1/(gh)^\beta), \beta\in N$	$(S_g^\beta S_h^\beta)(M(\mathscr{G},g,h))\|_{g=1=h}$
SDD	g^2+b^2/gh	$(D_gS_h+D_hS_g)(M(\mathscr{G},g,h))\|_{g=1=h}$

Table 2: Some other TIs from M-polynomial.

Indices	$f(g,h)$	Derivation from $M(\mathscr{G},g,h)$
H	$2/g+h$	$2S_gJ(M(\mathscr{G},g,h))\|_{g=1=h}$
IS	$gh/g+h$	$S_gQ_2JD_gD_h(M(\mathscr{G},g,h))\|_{g=1=h}$
AZI	$(gh/g+h-2)^3$	$S_g^3JD_g^3D_h^3(M(\mathscr{G},g,h))\|_{g=1=h}$

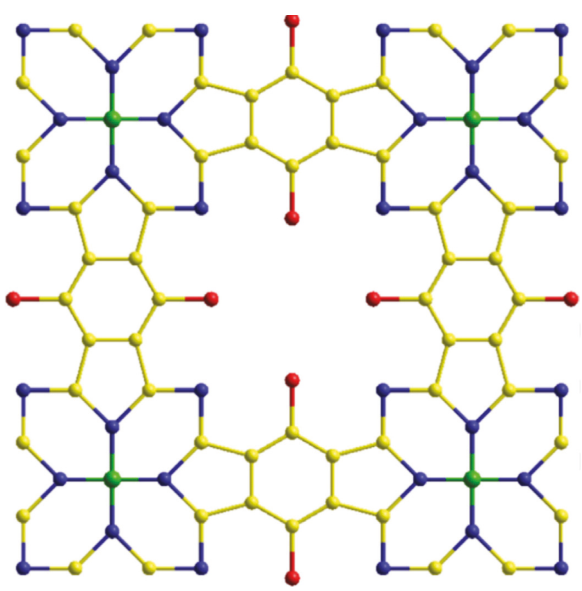

Figure 1: Transition metal tetra-cyano-benzene organic network.

MON of TM-TCNB is shown in Figure 1 which represents four colors consisting of blue, cyano, red, and yellow, representing N, TM, H, and N, respectively. Therefore, N stands for nitrogen, TM for transition metals, H for hydrogen, and C for carbon atom. The degree-based TI is a modern tool that opens up exciting discussion for many networks in the field of degree-based TIs. The modern contribution of these TIs based on degree is to compute the exact form of more than ten degrees and connection number-based descriptors.

Now, we take TM-TCNB as the primary network, and it does not recognize double or triple bonds (that is the primary reason to eliminate the hydrogen atoms). Furthermore, we eliminated eight hydrogen atoms from the network of TM-TCNB that were available at paranodes (vertices) of every benzene ring (present at the middle of every metal). After eliminating hydrogen's atoms from the middle of the benzene ring, the rest of the network is presented as $(\text{TM-TCNB})^1$, and this is our first metal-organic network. After that, we are going through the importance of the gained network of $(\text{TM-TCNB})^1$. So, we are left at the point to add four new benzene rings (adjacent to middle benzene into first network $(\text{TM-TCNB})^1$). Now, the resultant structure is TM-TCNB^2, and we know it as our second metal-organic network, as shown in Figure 2.

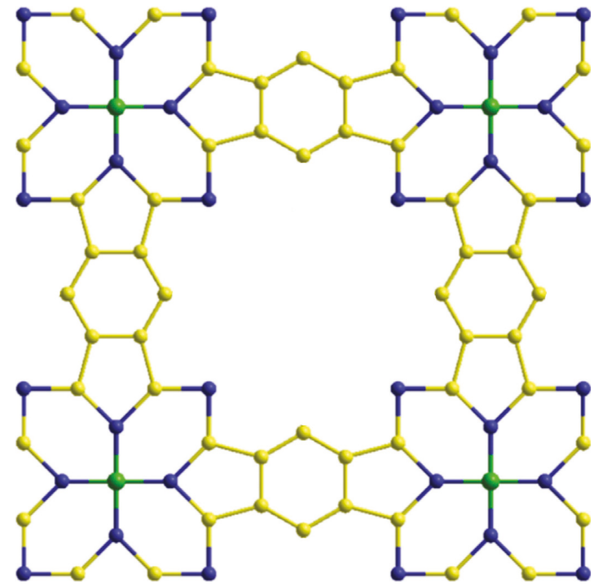

Figure 2: Transition metal tetra-cyano-benzene organic network type-I.

3. Main Results

In this section, we find the M-polynomial and different TIs with the help of this M-polynomial for the of the transition metal tetra-cyano-benzene organic network type-I $(\text{TM-TCNB})^1$ and type-II $(\text{TM-TCNB})^2$.

Theorem 1. *Let $\mathscr{G}_1=(TM-TCNB)^1$ be a transition metal tetra-cyano-benzene organic network type-I. Then, the M-polynomial of $\mathscr{G}_1$ is*

$$M(\mathscr{G}_1,g,h)=(8z+8)g^2h^2+(56z-8)g^2h^3 + (60z-20)g^3h^3+(16z)g^3h^4. \quad (8)$$

Proof. From Figure 2, we note that 3 distinct types of vertices exist in $(\text{TM-TCNB})^1$ as follows:

$$\begin{aligned} V_1 &= \{x\in V(\mathscr{G}_1)|\varphi(x)=2\},\\ V_2 &= \{x\in V(\mathscr{G}_1)|\varphi(x)=3\},\\ V_3 &= \{x\in V(\mathscr{G}_1)|\varphi(x)=4\}, \end{aligned} \quad (9)$$

such that

$$\begin{aligned}|V_1| &= 36z + 4,\\ |V_2| &= 64z - 16,\\ |V_3| &= 4z.\end{aligned} \quad (10)$$

Moreover,

$$|V(\mathrm{TM-TCNB})_1(n)| = |V_1| + |V_2| + |V_3| = 104z - 12. \quad (11)$$

We have 4 distinct types of edges that is based on the degrees of end vertices in $\mathcal{G}_1$ that are $\{2,2\}, \{2,3\}, \{3,3\}, \{3,4\}$, such that

$$\begin{aligned}E_{2,2} &= \{e = xy \in E(\mathcal{G}_1) | \varphi(x) = 2, \varphi(y) = 2\},\\ E_{2,3} &= \{e = xy \in E(\mathcal{G}_1) | \varphi(x) = 2, \varphi(y) = 3\},\\ E_{3,3} &= \{e = xy \in E(\mathcal{G}_1) | \varphi(x) = 3, \varphi(y) = 3\},\\ E_{3,4} &= \{e = xy \in E(\mathcal{G}_1) | \varphi(x) = 3, \varphi(y) = 4\} \text{with}\\ |E_1| &= 8z + 8,\\ |E_2| &= 56z - 8,\\ |E_3| &= 60z - 20,\\ |E_4| &= 16z.\end{aligned}$$

Moreover, $|E(\mathcal{G}_1)| = |E_1| + |E_2| + |E_3| + |E_4| = 140z - 20.$ (12)

Now, the partition of the vertex set and edge set of the type-1 MON are given in Tables 3 and 4.

Now, by using definitions of M-polynomial Tables 3 and 4, we have

$$\begin{aligned}M(\mathcal{G}_1, g, h) &= \sum_{s \le t} \left[|E_{s,t}(\mathcal{G}_1)| g^s h^t \right]\\ &= \sum_{2 \le 2} \left[|E_{2,2}(\mathcal{G}_1)| g^2 h^2 \right]\\ &\quad + \sum_{2 \le 3} \left[|E_{2,3}(\mathcal{G}_1)| g^2 h^3 \right]\\ &\quad + \sum_{3 \le 3} \left[|E_{3,3}(\mathcal{G}_1)| g^3 h^3 \right]\\ &\quad + \sum_{3 \le 4} \left[|E_{3,4}(\mathcal{G}_1)| g^3 h^4 \right] = |E_1| g^2 h^2 + |E_2| g^2 h^3\\ &\quad + |E_3| g^3 h^3 + |E_4| g^3 h^4\\ &= (8z + 8) g^2 h^2 + (56z - 8) g^2 h^3\\ &\quad + (60z - 20) g^3 h^3 + (16z) g^3 h^4.\end{aligned} \quad (13)$$

□

Table 3: The partition of the vertex set of $(\mathrm{TM-TCNB})^1$.

Vertex partition	V_1	V_2	V_3
Cardinality	$36z + 4$	$64z - 16$	$4z$

Table 4: The partition of the edge set of $(\mathrm{TM-TCNB})^1$.

Edge partition	E_1	E_2	E_3	E_4
Cardinality	$8z + 8$	$56z - 8$	$60z - 20$	$16z$

Theorem 2. *Let $\mathcal{G}_1 = (TM - TCNB)^1$ be the transition metal tetra-cyano-benzene organic network type-I. Then,*

$$\begin{aligned}M_1(\mathcal{G}_1) &= 784z - 128,\\ M_2(\mathcal{G}_1) &= 1100z - 196,\\ \mathrm{MM}_2(\mathcal{G}_1) &= 20z - \frac{14}{9},\\ R_\beta(\mathcal{G}_1) &= (4)^\beta (8z + 8) + (16)^\beta (56z - 8)\\ &\quad + (9)^\beta (60z - 20) + (12)^\beta (16z),\\ \mathrm{RR}_\beta(\mathcal{G}_1) &= \frac{1}{(4)^\beta}(8z + 8) + \frac{1}{(6)^\beta}(56z - 8)\\ &\quad + \frac{1}{(9)^\beta}(60z - 20) + \frac{1}{(12)^\beta}(16z),\\ \mathrm{SDD}(\mathcal{G}_1) &= \left(\frac{872}{3}\right) z - \frac{124}{3}.\end{aligned} \quad (14)$$

Proof. Let $f(g,h) = M(\mathcal{G}_1, g, h)$ be the M-polynomial of the type-1 (Theorem 1) MON; then,

$$\begin{aligned}f(g,h) &= (8z + 8) g^2 h^2 + (56z - 8) g^2 h^3\\ &\quad + (60z - 20) g^3 h^3 + (16z) g^3 h^4.\end{aligned} \quad (15)$$

First, we find the required partial derivatives and integrals as

$$\begin{aligned}
D_g(f(g,h)) &= \frac{\partial(f(g,h))}{\partial g}\\
&= 2(8z+8)gh^2 + 2(56z-8)gh^3 + 3(60z-20)g^2h^3 + 3(16z)g^2h^4,\\
D_h(f(g,h)) &= \frac{\partial(f(g,h))}{\partial h}\\
&= 2(8z+8)g^2h + 3(56z-8)g^2h^2 + 3(60z-20)g^3h^2 + 4(16z)g^3h^3,\\
D_g(D_h(f(g,h))) &= 4(8z+8)gh + 6(56z-8)gh^2 + 9(60z-20)g^2h^2 + 12(16z)g^2h^3,\\
T_g(f(g,h)) &= \int_0^g \frac{f(u,h)}{u}\mathrm{d}u\\
f(u,h) &= (8z+8)u^2h^2 + (56z-8)u^2h^3 + (60z-20)u^3h^3 + (16z)u^3h^4\\
\frac{f(u,h)}{u} &= (8z+8)uh^2 + (56z-8)uh^3 + (60z-20)u^2h^3 + (16z)u^2h^4\\
\int_0^g \frac{f(u,h)}{u}\mathrm{d}u &= \left|\frac{(8z+8)}{2}u^2h^2 + \frac{1}{2}(56z-8)u^2h^3 + \frac{1}{3}(60z-20)u^3h^3 + \frac{1}{3}(16z)u^3h^4\right|_0^g\\
&= \frac{1}{2}(8z+8)g^2h^2 + \frac{1}{2}(56z-8)g^2h^3 + \frac{1}{3}(60z-20)g^3h^3 + \frac{1}{3}(16z)g^3h^4,\\
T_h(f(g,h)) &= \int_0^h \frac{f(g,u)}{u}\mathrm{d}u\\
f(g,u) &= (8z+8)g^2u^2 + (56z-8)g^2u^3 + (60z-20)g^3u^3 + (16z)g^3u^4\\
\frac{f(g,u)}{u} &= (8z+8)g^2u + (56z-8)g^2u^2 + (60z-20)g^3u^2 + (16z)g^3u^3\\
\int_0^h \frac{f(g,u)}{u}\mathrm{d}u &= \left|\frac{1}{2}(8z+8)g^2u^2 + \frac{1}{3}(56z-8)g^2u^3 + \frac{1}{3}(60z-20)g^3u^3 + \frac{1}{4}(16z)g^3u^4\right|_0^h\\
&= \frac{1}{2}(8z+8)g^2h^2 + \frac{1}{3}(56z-8)g^2h^3 + \frac{1}{3}(60z-20)g^3h^3 + \frac{1}{4}(16z)g^3h^4,\\
T_gT_h(f(g,h)) &= T_g(T_h(f(g,h)))\\
&= \frac{1}{2}(8z+8)u^2h^2 + \frac{1}{3}(56z-8)u^2h^3 + \frac{1}{3}(60z-20)u^3h^3 + \frac{1}{4}(16z)u^3h^4\\
&= \frac{1}{2}(8z+8)uh^2 + \frac{1}{3}(56z-8)uh^3 + \frac{1}{3}(60z-20)u^2h^3 + \frac{1}{4}(16z)u^2h^4\\
&= \left|\frac{1}{4}(8z+8)u^2h^2 + \frac{1}{6}(56z-8)u^2h^3 + \frac{1}{9}(60z-20)u^3h^3 + \frac{1}{8}(16z)u^3h^4\right|_0^g\\
&= \frac{1}{4}(8z+8)g^2h^2 + \frac{1}{6}(56z-8)g^2h^3 + \frac{1}{9}(60z-20)g^3h^3 + \frac{1}{8}(16z)g^3h^4,\\
D_h\left(T_g(f(g,h))\right) &= D_h\left[\frac{1}{2}(8z+8)g^2h^2 + \frac{1}{2}(56z-8)g^2h^3 + \frac{1}{3}(60z-20)g^3h^3 + \frac{1}{3}(16z)g^3h^4\right]\\
&= \frac{2}{2}(8z+8)g^2h + \frac{3}{2}(56z-8)g^2h^2 + \frac{3}{3}(60z-20)g^3h^2 + \frac{4}{3}(16z)g^3h^3\\
&= (8z+8)g^2h + \frac{3}{2}(56z-8)g^2h^2 + (60z-20)g^3h^2 + \frac{4}{3}(16z)g^3h^3,\\
D_g\left(T_h(f(g,h))\right) &= D_g\left[\frac{1}{2}(8z+8)g^2h^2 + \frac{1}{3}(56z-8)g^2h^3 + \frac{1}{3}(60z-20)g^3h^3 + \frac{1}{4}(16z)g^3h^4\right]\\
&= (8z+8)gh^2 + \frac{2}{3}(56z-8)gh^3 + (60z-20)g^2h^3 + \frac{3}{4}(16z)g^3h^3.\\
D_g^{\beta}\left(D_h^{\beta}(f(g,h))\right) &= (4)^{\beta}(8z+8) + (6)^{\beta}(56z-8)gh^2 + (9)^{\beta}(60z-20)g^2h^2\\
&\quad + (12)^{\beta}(16z)g^2h^3\\
T_g^{\beta}\left(T_h^{\beta}(f(g,h))\right) &= \frac{(8z+8)}{(4)^{\beta}}g^2h^2 + \frac{1}{(6)^{\beta}}(56z-8)g^2h^3 + \frac{1}{(9)^{\beta}}(60z-20)g^3h^3,\\
&\quad + \frac{1}{(12)^{\beta}}(16z)g^3h^4.
\end{aligned}\tag{16}$$

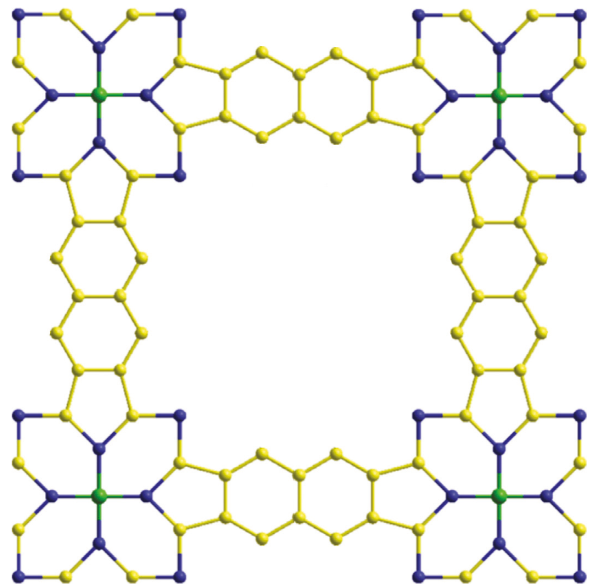

Figure 3: Transition metal tetra-cyano-benzene organic network type-II.

Now, by substituting $h = g = 1$,

$$
\begin{aligned}
D_g(f(g,h))_{g=1=h} &= 356z - 60,\\
D_h(f(g,h))_{g=1=h} &= 428z - 68,\\
D_g(D_h(f(g,h)))_{g=1=h} &= 1100z - 196,\\
T_g(f(g,h))_{g=1=h} &= \left(\frac{172}{3}\right)z - \frac{20}{3},\\
T_h(f(g,h))_{g=1=h} &= \left(\frac{140}{3}\right)z - \frac{16}{3},\\
T_gT_h(f(g,h))_{g=1=h} &= 20z - \frac{14}{9},\\
D_h\left(T_g(f(g,h))\right)_{g=1=h} &= \left(\frac{520}{3}\right)z - 24,\\
D_g(T_h(f(g,h)))_{g=1=h} &= \left(\frac{352}{3}\right)z - \frac{52}{3},\\
D_g^{\beta}\left(D_h^{\beta}(f(g,h))\right)_{g=1=h} &= (4)^{\beta}(8z+8) + (6)^{\beta}(56z-8)\\
&\quad + (9)^{\beta}(60z-20) + (12)^{\beta}(16z),\\
T_g^{\beta}\left(T_h^{\beta}(f(g,h))\right)_{g=1=h} &= \frac{(8z+8)}{(4)^{\beta}} + \frac{1}{(6)^{\beta}}(56z-8)\\
&\quad + \frac{1}{(9)^{\beta}}(60z-20) + \frac{1}{(12)^{\beta}}(16z).
\end{aligned}
\tag{17}
$$

Using these values in formulae of Table 1,

$$
\begin{aligned}
M_1(\mathscr{G}_1) &= \left(D_g + D_h\right)f(g,h)_{g=1=h}\\
&= D_gf(g,h)_{g=1=h} + D_hf(g,h)_{g=1=h}\\
&= 784z - 128,\\
M_2(\mathscr{G}_1) &= D_gD_hf(g,h)_{g=1=h}\\
&= D_g(D_hf(g,h))_{g=1=h} = 1100z - 196,\\
\mathrm{MM}_2(\mathscr{G}_1) &= T_g(T_h(f(g,h)))_{g=1=h} = 20z - \frac{14}{9},\\
R_{\beta}(\mathscr{G}_1) &= D_g^{\beta}\left(D_h^{\beta}(f(g,h))\right)_{g=1=h}\\
&= (4)^{\beta}(8z+8) + (6)^{\beta}(56z-8)\\
&\quad + (9)^{\beta}(60z-20) + (12)^{\beta}(16z),\\
\mathrm{RR}_{\beta}(\mathscr{G}_1) &= T_g^{\beta}\left(T_h^{\beta}(f(g,h))\right)_{g=1=h}\\
&= \frac{(8z+8)}{(4)^{\beta}} + \frac{1}{(6)^{\beta}}(56z-8)\\
&\quad + \frac{1}{(9)^{\beta}}(60z-20) + \frac{1}{(12)^{\beta}}(16z),\\
\mathrm{SDD}(\mathscr{G}_1) &= \left|D_gT_h + D_hT_g\right|f(g,h)_{g=1=h}\\
&= D_gT_hf(g,h)_{g=1=h} + D_hT_gf(g,h)_{g=1=h}\\
&= \left(\frac{872}{3}\right)z - \frac{124}{3}.
\end{aligned}
\tag{18}
$$

□

Theorem 3. *Let $\mathscr{G}_1 = (TM - TCNB)^1$ be the transition metal tetra-cyano-benzene organic network type-I. Then,*

$$
\begin{aligned}
H(\mathscr{G}_1) &= \frac{1784}{35}z - \frac{88}{15},\\
\mathrm{IS}(\mathscr{G}_1) &= \frac{6742}{35}z - \frac{158}{5},\\
\mathrm{AZI}(\mathscr{G}_1) &= \frac{103763}{5}z - 3965.
\end{aligned}
\tag{19}
$$

Proof. Let $f(g,h) = M(\mathscr{G}_1, g, h)$ be the M-polynomial of MON; then,

$$
\begin{aligned}
M(\mathscr{G}_1, g, h) &= (8z+8)g^2h^2 + (56z-8)g^2h^3 + (60z-20)g^3h^3 + (16z)g^3h^4 \\
J(f(g,h)) &= (8z+8)g^4 + (56z-8)g^5 + (60z-20)g^6 + (16z)g^7 \\
S_g(J(f(g,h))) &= \frac{1}{4}(8z+8)g^4 + \frac{1}{5}(56z-8)g^5 + \frac{1}{6}(60z-20)g^6 + \frac{1}{7}(16z)g^7 \\
J\big(D_g(D_h(f(g,h)))\big) &= 4(8z+8)g^2 + 6(56z-8)g^3 + 9(60z-20)g^4 + 12(16z)g^8 \\
Q_2\Big(J\big(D_g(D_h(f(g,h)))\big)\Big) &= 4(8z+8)g^4 + 6(56z-8)g^5 \\
&\quad + 9(60z-20)g^6 + 12(16z)g^7 \\
S_g\Big(Q_2\Big(J\big(D_g(D_h(f(g,h)))\big)\Big)\Big) &= (8z+8)g^4 + \frac{6}{5}(56z-8)g^5 \\
&\quad + \frac{9}{6}(60z-20)g^6 + \frac{12}{7}(16z)g^7 \\
J\big(D_g^3\big(D_h^3(f(g,h))\big)\big) &= (4)^3(8z+8)g^2 + (6)^3(56z-8)g^3 \\
&\quad + (9)^3(60z-20)g^4 + (12)^3(16z)g^5 \\
S_g^3\Big(J\big(D_g^3\big(D_h^3(f(g,h))\big)\big)\Big) &= \left(\frac{4}{2}\right)^3(8z+8)g^2 + \left(\frac{6}{3}\right)^3(56z-8)g^3 \\
&\quad + \left(\frac{9}{4}\right)^3(60z-20)g^4 + \left(\frac{12}{5}\right)^3(16z)g^5 \\
S_g(J(f(g,h)))_{g=1=h} &= \frac{892}{35}z - \frac{44}{15} \\
S_g\Big(Q_2\Big(J\big(D_g(D_h(f(g,h)))\big)\Big)\Big)_{g=1=h} &= \left(\frac{6742}{35}\right)z - \frac{158}{5} \\
S_g^3\Big(J\big(D_g^3\big(D_h^3(f(g,h))\big)\big)\Big)_{g=1=h} &= \frac{103763}{5}z = 3965 \\
J(f(g,h)) &= Jf(g,h) = (8z+8)g^4 + (56z-8)g^5 + (60z-20)g^6 + (16z)g^5 \\
S_g(J(f(g,h))) &= \int_0^g \frac{f(J(f(g,h)))}{u}\,\mathrm{d}u \\
&= \int_0^g \frac{(8z+8)u^4 + (56z-8)u^5 + (60z-20)u^6 + (16z)u^7}{u}\,\mathrm{d}u \\
&= \int_0^g (8z+8)u^3 + (56z-8)u^4 + (60z-20)u^5 + (16z)u^7\,\mathrm{d}u \\
&= \left|\frac{(8z+8)u^4}{4} + \frac{1}{5}(56z-8)u^5 + \frac{1}{6}(60z-20)u^6 + \frac{(16z)}{7}u^7\right|_0^g \\
&= \frac{(8z+8)g^4}{4} + \frac{1}{5}(56z-8)g^5 + \frac{1}{6}(60z-20)g^6 + \frac{(16z)}{7}g^7 \\
J\big(D_g(D_h(f(g,h)))\big) &= 4(8z+8)g^2 + 6(56z-8)g^3 + 9(60z-20)g^4 + 12(16z)g^5 \\
Q_2\Big(J\big(D_g(D_h(f(g,h)))\big)\Big) &= Q_2\left[4(8z+8)g^2 + 6(56z-8)g^3 + 9(60z-20)g^4 + 12(16z)g^5\right] \\
&= 4(8z+8)g^4 + 6(56z-8)g^5 + 9(60z-20)g^6 + 12(16z)g^7 \\
S_g\Big(Q_2\Big(J\big(D_g(D_h(f(g,h)))\big)\Big)\Big) &= S_g\left[4(8z+8)g^4 + 6(56z-8)g^5 + 9(60z-20)g^6 + 12(16z)g^7\right] \\
&= \int_0^g \left[4(8z+8)u^3 + 6(56z-8)u^4 + 9(60z-20)u^5 + 12(16z)u^6\right]\mathrm{d}u \\
&= \left|\frac{4}{4}(8z+8)u^4 + \frac{6}{5}(56z-8)u^5 + \frac{9}{6}(60z-20)u^6 + \frac{12}{7}(16z)u^7\right|_0^g \\
&= (8z+8)g^4 + \frac{6}{5}(56z-8)g^5 + \frac{3}{2}(60z-20)g^6 + \frac{12}{7}(16z)g^7 \\
J\big(D_g^3\big(D_h^3(f(g,h))\big)\big) &= (4)^3(8z+8)g^2 + (6)^3(56z-8)g^3 + (9)^3(60z-20)g^4 + (12)^3(16z)g^5 \\
S_g^3\Big(J\big(D_g^3\big(D_h^3(f(g,h))\big)\big)\Big) &= (4)^3(8z+8)u^2 + (6)^3(56z-8)u^3 \\
&\quad + (9)^3(60z-20)u^4 + (12)^3(16z)u^5 \\
&= \int_0^g \left|(4)^3(8z+8)u + (6)^3(56z-8)u^2 + (9)^3(60z-20)u^3 + (12)^3(16z)u^4\right|\mathrm{d}u \\
&= \left|\frac{64}{2}(8z+8)u^2 + \frac{216}{3}(56z-8)u^3 + \frac{729}{4}(60z-20)u^4 + \frac{1728}{5}(16z)u^5\right|_0^g \\
&= \frac{64}{2}(8z+8)g^2 + \frac{216}{3}(56z-8)g^3 + \frac{729}{4}(60z-20)g^4 + \frac{1728}{5}(16z)g^5,
\end{aligned}
\tag{20}
$$

therefore,

$$
\begin{aligned}
S_g(J(f(g,h)))_{g=1=h} &= \frac{1}{4}(8z+8)+\frac{1}{5}(56z-8)+\frac{1}{6}(60z-20)+\frac{16}{7}z\\
&= \frac{892}{35}z-\frac{44}{15},\\
S_g\Big(Q_2\Big(J\Big(D_g\left(D_h\left(f(g,h)\right)\right)\Big)\Big)\Big)_{g=1=h} &= (8z+8)+\frac{6}{5}(56z-8)+\frac{3}{2}(60z-20)+\frac{12}{7}(16z)\\
&= \left(\frac{6742}{35}\right)z-\frac{158}{5},\\
S_g^3\Big(J\Big(D_g^3\Big(D_h^3\left(f(g,h)\right)\Big)\Big)\Big)_{g=1=h} &= \frac{64}{2}(8z+8)+\frac{216}{3}(56z-8)+\frac{729}{4}(60z-20)+\frac{1728}{5}(16z)\\
&= \frac{103763}{5}z-3965,\\
H(\mathcal{G}_1) &= 2S_g(J(f(g,h)))_{g=1=h}\\
&= 2\left\{\left(\frac{892}{35}\right)z-\frac{44}{15}\right\}=\frac{1784}{35}z-\frac{88}{15},\\
\mathrm{IS}(\mathcal{G}_1) &= S_g\Big(Q_2\Big(J\Big(D_g\left(D_h\left(f(g,h)\right)\right)\Big)\Big)\Big)_{g=1=h}=\frac{6742}{35}z-\frac{158}{5},\\
\mathrm{AZI}(\mathcal{G}_1) &= S_g^3\Big(J\Big(D_g^3\Big(D_h^3\left(f(g,h)\right)\Big)\Big)\Big)_{g=1=h}=\frac{103763}{5}z-3965.
\end{aligned}
\tag{21}
$$

□

Theorem 4. *Let $\mathcal{G}_2=(TM-TCNB)^2$ be the transition metal tetra-cyano-benzene organic network type-II. Then, the M-polynomial of $\mathcal{G}_2$ is*

$$
\begin{aligned}
M(\mathcal{G}_2,g,h) &= 8(z+1)g^2h^2+16(5z-1)g^2h^3\\
&\quad +11(6z-2)g^3h^3+(16z)g^3h^4.
\end{aligned}
\tag{22}
$$

Proof. From Figure 3, we show the partition of the vertex set and the edge set of $\mathcal{G}_2$ according to degrees of the vertices. In this way, we get 3 distinct types of vertices in $\mathcal{G}_2$ as follows:

$$
\begin{aligned}
V_1 &= \{x\in V(\mathcal{G}_2)|\varphi(x)=2\},\\
V_2 &= \{x\in V(\mathcal{G}_2)|\varphi(x)=3\},\\
V_3 &= \{x\in V(\mathcal{G}_2)|\varphi(x)=4\},
\end{aligned}
\tag{23}
$$

such that

$$
\begin{aligned}
|V_1| &= 48z,\\
|V_2| &= 56z-20,\\
|V_3| &= 4z.
\end{aligned}
\tag{24}
$$

Also,

$$
|\mathcal{G}_2| = x = |V_1|+|V_2|+|V_3| = 128z-20. \tag{25}
$$

Now, we get distinct types of edges based on the degree of end vertices of $\mathcal{G}_2$ that are

$$
\begin{aligned}
&\{2,2\},\{2,3\},\{3,3\}\&\{3,4\}\\
E_{2,2} &= \{e=xy\in E(\mathcal{G}_2)|\varphi(x)=2,\varphi(y)=2\},\\
E_{2,3} &= \{e=xy\in E(\mathcal{G}_2)|\varphi(x)=2,\varphi(y)=3\},\\
E_{3,3} &= \{e=xy\in E(\mathcal{G}_2)|\varphi(x)=3,\varphi(y)=3\},\\
E_{3,4} &= \{e=xy\in E(\mathcal{G}_2)|\varphi(x)=3,\varphi(y)=4\}\text{with}\\
E|\mathcal{G}_2| &= e = |E_{2,2}|+|E_{2,3}|+|E_{3,3}|+|E_{3,4}| = 170z-30.
\end{aligned}
\tag{26}
$$

Table 5: The partition of the vertex set of $(\mathrm{TM}-\mathrm{TCNB})^2$.

Vertex partition	V_1	V_2	V_3
Cardinality	$48z$	$76z-20$	$4z$

Table 6: The partition of the edge set of $(\mathrm{TM}-\mathrm{TCNB})^2$.

Edge partition	$E_{2,2}$	$E_{2,3}$	$E_{3,3}$	$E_{3,4}$
Cardinality	$8(z+1)$	$16(5z-1)$	$11(6z-2)$	$16z$

Therefore, partition of the vertex set and the edge set of the metal-organic network $(\mathrm{TM}-\mathrm{TCNB})^2$ are given in Tables 5 and 6.

By using definition of M-polynomial, Tables 5 and 6, we have

$$\begin{aligned}
M(\mathscr{G}_2,g,h) &= \sum_{s\le t}\left[|E_{s,t}(\mathscr{G}_2)|g^s h^t\right]\\
&= \sum_{2\le 2}\left[|E_{2,2}(\mathscr{G}_2)|g^2h^2\right]+\sum_{2\le 3}\left[|E_{2,3}(\mathscr{G}_2)|g^2h^3\right]\\
&\quad+\sum_{3\le 3}\left[|E_{3,3}(\mathscr{G}_2)|g^3h^3\right]+\sum_{3\le 4}\left[|E_{3,4}(\mathscr{G}_2)|g^3h^4\right]\\
&=|E_1|g^2h^2+|E_2|g^2h^3+|E_3|g^3h^3+|E_4|g^3h^4.\\
M(\mathscr{G}_2,g,h) &= 8(z+1)g^2h^2+16(5z-1)g^2h^3+11(6z-2)g^3h^3+(16z)g^3h^4.
\end{aligned} \tag{27}$$

□

Theorem 5. *Let $\mathscr{G}_2=(TM-TCNB)^2$ be a transition metal tetra-cyano-benzene organic network type-II. Then,*

$$\begin{aligned}
M_1(\mathscr{G}_2) &= 940z-180,\\
M_2(\mathscr{G}_2) &= 1298z-98,\\
\mathrm{MM}_2(\mathscr{G}_2) &= 24z-\frac{28}{9},\\
R_\beta(\mathscr{G}_2) &= (4)^\beta 8(z+1)+(6)^\beta 16(5z-1)+(9)^\beta 11(6z-2)+(12)^\beta(16z),\\
\mathrm{RR}_\beta(\mathscr{G}_2) &= \frac{8}{(4)^\beta}(z+1)+\frac{16}{(6)^\beta}(5z-1)+\frac{11}{(9)^\beta}(6z-2)+\frac{1}{(12)^\beta}(16z).
\end{aligned} \tag{28}$$

Proof. Let $f(g,h)=M(\mathscr{G}_2,g,h)$ be the M-polynomial of second MON:

$$\begin{aligned}
M(\mathscr{G}_2,g,h) &= 8(z+1)g^2h^2+16(5z-1)g^2h^3\\
&\quad+11(6z-2)g^3h^3+(16z)g^3h^4.
\end{aligned} \tag{29}$$

The needed derivatives and integrals are calculated as

$$
\begin{aligned}
D_g(f(g,h)) &= \frac{\partial(f(g,h))}{\partial g}\\
&= 16(z+1)gh^2 + 32(5z-1)gh^3 + 33(6z-2)g^2h^3 + 3(16z)g^2h^4\\
D_g(f(g,h))_{g=1=h} &= 16(z+1) + 32(5z-1) + 33(6z-2) + 3(16z) = 422z - 82,\\
D_h(f(g,h)) &= \frac{\partial(f(g,h))}{\partial h} = 16(z+1)g^2h + 48(5z-1)g^2h^2 + 33(6z-2)g^3h^2 + 4(16z)g^2h^3\\
D_h(f(g,h))_{g=1=h} &= 16(z+1) + 48(5z-1) + 33(6z-2) + 4(16z) = 518z - 98,\\
D_g(D_h(f(g,h))) &= 32(z+1)gh + 96(5z-1)gh^2 + 99(6z-2)g^2h^2 + 12(16z)g^2h^3\\
D_g(D_h(f(g,h)))_{g=1=h} &= 32(z+1) + 96(5z-1) + 99(6z-2) + 12(16z) = 1298z - 262,\\
S_g(f(g,h)) &= \int_0^g \frac{f(u,h)}{u}\,\mathrm{d}u\\
&= \int_0^g \frac{8(z+1)u^2h^2 + 16(5z-1)u^2h^3 + 11(6z-2)u^3h^3 + (16z)u^3h^4}{u}\,\mathrm{d}u\\
\int_0^g \frac{f(u,h)}{u}\,\mathrm{d}u &= \left|\frac{8(z+1)}{2}u^2h^2 + \frac{16}{2}(5z-1)u^2h^3 + \frac{11}{3}(6z-2)u^3h^3 + \frac{1}{3}(16z)u^3h^4\right|_0^g\\
&= \frac{8}{2}(z+1)g^2h^2 + \frac{16}{2}(5z-1)g^2h^3 + \frac{11}{3}(6z-2)g^3h^3 + \frac{1}{3}(16z)g^3h^4,\\
S_g(f(g,h))_{g=1=h} &= \frac{8}{2}(z+1) + \frac{16}{2}(5z-1) + \frac{11}{3}(6z-2) + \frac{1}{3}(16z) = \frac{214}{3}z - \frac{34}{3},\\
S_h(f(g,h)) &= \int_0^h \frac{f(g,u)}{u}\,\mathrm{d}u\\
f(g,u) &= 8(z+1)g^2u^2 + 16(5z-1)g^2u^3 + 11(6z-2)g^3u^3 + (16z)g^3u^4\\
\frac{f(g,u)}{u} &= 8(z+1)g^2u + 16(5z-1)g^2u^2 + 11(6z-2)g^3u^2 + (16z)g^3u^3\\
\int_0^h \frac{f(g,u)}{u}\,\mathrm{d}u &= \left|\frac{8}{2}(z+1)g^2u^2 + \frac{16}{3}(5z-1)g^2u^3 + \frac{11}{3}(6z-2)g^3u^3 + \frac{1}{4}(16z)g^3u^4\right|_0^h\\
&= \frac{8}{2}(z+1)g^2h^2 + \frac{16}{3}(5z-1)g^2h^3 + \frac{11}{3}(6z-2)g^3h^3 + \frac{1}{4}(16z)g^3h^4\\
S_h(f(g,h))_{g=1=h} &= \frac{8}{2}(z+1) + \frac{16}{3}(5z-1) + \frac{11}{3}(6z-2) + \frac{1}{4}(16z) = \frac{170}{3}z - \frac{26}{3},\\
S_gS_h(f(g,h)) &= S_g(S_h(f(g,h)))\\
&= 2(z+1)g^2h^2 + \frac{8}{3}(5z-1)g^2h^3 + \frac{11}{9}(6z-2)g^3h^3 + \frac{1}{12}(16z)g^3h^4\\
S_gS_h(f(g,h))_{g=1=h} &= 2(z+1) + \frac{8}{3}(5z-1) + \frac{11}{9}(6z-2) + \frac{1}{12}(16z) = 24z - \frac{28}{9},\\
D_h(S_g(f(g,h))) &= D_h\left[\frac{8}{2}(z+1)g^2h^2 + \frac{16}{2}(5z-1)g^2h^3 + \frac{11}{3}(6z-2)g^3h^3 + \frac{1}{3}(16z)g^3h^4\right]\\
&= \frac{2(8)}{2}(z+1)g^2h + \frac{3(16)}{2}(5z-1)g^2h^2 + \frac{3(11)}{3}(6z-2)g^3h^2 + \frac{4}{3}(16z)g^3h^3\\
&= 8(z+1)g^2h + 24(5z-1)g^2h^2 + 11(6z-2)g^3h^2 + \frac{4}{3}(16z)g^3h^3\\
D_h(S_g(f(g,h)))_{g=1=h} &= 8(z+1) + 24(5z-1) + 11(6z-2) + \frac{4}{3}(16z) = \frac{646}{3}z - 38,\\
D_g(S_h(f(g,h))) &= D_g\left[\frac{8}{2}(z+1)g^2h^2 + \frac{16}{3}(5z-1)g^2h^3 + \frac{11}{3}(6z-2)g^3h^3 + \frac{1}{4}(16z)g^3h^4\right]\\
&= 8(z+1)gh^2 + \frac{32}{3}(5z-1)gh^3 + 11(6z-2)g^2h^3 + \frac{3}{4}(16z)g^2h^4\\
D_g(S_h(f(g,h)))_{g=1=h} &= 8(z+1) + \frac{32}{3}(5z-1) + 11(6z-2) + \frac{3}{4}(16z) = \frac{418}{3}z - \frac{74}{3},\\
D_g^\beta(D_h^\beta(f(g,h))) &= (4)^\beta 8(z+1)gh + (6)^\beta(16)(5z-1)gh^2 + (9)^\beta(11)(6z-2)g^2h^2 + (12)^\beta(16z)g^2h^3\\
D_g^\beta(D_h^\beta(f(g,h)))_{g=1=h} &= (4)^\beta 8(z+) + (6)^\beta(16)(5z-1) + (9)^\beta(11)(6z-2) + (12)^\beta(16z)\\
S_g^\beta(S_h^\beta(f(g,h))) &= \frac{8(z+1)}{(4)^\beta}g^2h^2 + \frac{16}{(6)^\beta}(5z-1)g^2h^3 + \frac{11}{(9)^\beta}(6z-2)g^3h^3 + \frac{1}{(12)^\beta}(16z)g^3h^4\\
S_g^\beta(S_h^\beta(f(g,h)))_{g=1=h} &= \frac{8(z+1)}{(4)^\beta} + \frac{16}{(6)^\beta}(5z-1) + \frac{11}{(9)^\beta}(6z-2) + \frac{1}{(12)^\beta}(16z).
\end{aligned}
\tag{30}
$$

Now, by substituting $g = h = 1$,

$$\begin{aligned}
D_g(f(g,h))_{g=1=h} &= 422z - 82,\\
D_h(f(g,h))_{g=1=h} &= 518z - 98,\\
D_g(D_h(f(g,h)))_{g=1=h} &= 1298z - 262,\\
S_g(f(g,h))_{g=1=h} &= \frac{214}{3}z - \frac{34}{3},\\
S_h(f(g,h))_{g=1=h} &= \frac{170}{3}z - \frac{26}{3},\\
S_gS_h(f(g,h))_{g=1=h} &= 24z - \frac{28}{9},\\
D_h\big(S_g(f(g,h))\big)_{g=1=h} &= \frac{646}{3}z - 38,\\
D_g(S_h(f(g,h)))_{g=1=h} &= \frac{418}{3}z - \frac{74}{3},\\
D_g^{\beta}\big(D_h^{\beta}(f(g,h))\big)_{g=1=h} &= (4)^{\beta}8(z+1) + (6)^{\beta}(16)(5z-1) + (9)^{\beta}(11)(6z-2) + (12)^{\beta}(16z),\\
S_g^{\beta}\big(S_h^{\beta}(f(g,h))\big)_{g=1=h} &= \frac{8(z+1)}{(4)^{\beta}} + \frac{16}{(6)^{\beta}}(5z-1) + \frac{11}{(9)^{\beta}}(6z-2) + \frac{1}{(12)^{\beta}}(16z),\\
M_1(\mathcal{G}_2) &= \big(D_g + D_h\big)f(g,h)_{g=1=h}\\
&= D_g f(g,h)_{g=1=h} + D_h f(g,h)_{g=1=h} = 940z - 180,\\
M_2(\mathcal{G}_2) &= D_gD_h f(g,h)_{g=1=h}\\
&= D_g(D_h f(g,h))_{g=1=h} = 1298z - 98,\\
\mathrm{MM}_2(\mathcal{G}_2) &= S_g(S_h(f(g,h)))_{g=1=h} = 24z - \frac{28}{9},\\
R_{\beta}(\mathcal{G}_2) &= D_g^{\beta}\big(D_h^{\beta}(f(g,h))\big)_{g=1=h}\\
&= (4)^{\beta}(8)(z+1) + (6)^{\beta}(16)(5z-1) + (9)^{\beta}(11)(6z-2) + (12)^{\beta}(16z),\\
\mathrm{RR}_{\beta}(\mathcal{G}_2) &= S_g^{\beta}\big(S_h^{\beta}(f(g,h))\big)_{g=1=h} = \frac{8(z+1)}{(4)^{\beta}} + \frac{16}{(6)^{\beta}}(5z-1) + \frac{11}{(9)^{\beta}}(6z-2) + \frac{1}{(12)^{\beta}}(16z),\\
\mathrm{SDD}(\mathcal{G}_2) &= \big|D_gS_h + D_hS_g\big| f(g,h)_{g=1=h}\\
&= D_gS_h f(g,h)_{g=1=h} + D_hS_g f(g,h)_{g=1=h} = \left(\frac{1064}{3}\right)z - \frac{188}{3}.
\end{aligned} \tag{31}$$

□

Theorem 6. *Let $\mathcal{G}_2 = (TM - TCNB)^2$ be a transition metal tetra-cyano-benzene organic network type-II. Then,*

$$\begin{aligned}
H(\mathcal{G}_2) &= \frac{438}{7}z - \frac{146}{15},\\
\mathrm{IS}(\mathcal{G}_2) &= \frac{1613}{7}z - \frac{221}{5},\\
\mathrm{AZI}(\mathcal{G}_2) &= \frac{6707861}{4000}z - \frac{10067}{32}.
\end{aligned} \tag{32}$$

Proof. Let $f(g,h) = M(\mathcal{G}_2, g, h)$ be the M-polynomial of second MON; then,

$$
\begin{aligned}
M(\mathscr{G}_2, g, h) &= 8(z+1)g^2h^2 + 16(5z-1)g^2h^3 + 11(6z-2)g^3h^3 + (16z)g^3h^4,\\
J(f(g,h)) &= 8(z+1)g^4 + 16(5z-1)g^5 + 11(6z-2)g^6 + (16z)g^7,\\
S_g(J(f(g,h))) &= \frac{8}{4}(z+1)g^4 + \frac{16}{5}(5z-1)g^5 + \frac{11}{6}(6z-2)g^6 + \frac{1}{7}(16z)g^7,\\
J\big(D_g(D_h(f(g,h)))\big) &= 32(z+1)g^2 + 96(5z-1)g^3 + 99(6z-2)g^4 + 12(16z)g^5,\\
Q_2\big(J\big(D_g(D_h(f(g,h)))\big)\big) &= 32(z+1)g^4 + 96(5z-1)g^5 + 99(6z-2)g^6 + 12(16z)g^7,\\
S_g\big(Q_2\big(J\big(D_g(D_h(f(g,h)))\big)\big)\big) &= \frac{32}{4}(z+1)g^4 + \frac{96}{75}(5z-1)g^5 + \frac{99}{6}(6z-2)g^6 + \frac{12}{7}(16z)g^7\\
D_g^3\big(D_h^3(f(g,h))\big) &= (4)^3 8(z+1)gh + (16)^3(16)(5z-1)gh^2\\
&\quad + (9)^3(11)(6z-2)g^2h^2 + (12)^3(16z)g^2h^3,\\
J\big(D_g^3\big(D_h^3(f(g,h))\big)\big) &= (4)^3 8(z+1)g^2 + (16)^3(16)(5z-1)g^3\\
&\quad + (9)^3(11)(6z-2)g^4 + (12)^3(16z)g^5,\\
S_g^3\big(J\big(D_g^3\big(D_h^3(f(g,h))\big)\big)\big) &= \left(\frac{4}{2}\right)^3(8)(z+1)g^2 + \left(\frac{6}{3}\right)^3(16)(5z-1)g^3\\
&\quad + \left(\frac{9}{4}\right)^3(11)(6z-2)g^4 + \left(\frac{12}{5}\right)^3(16z)g^5,\\
S_g(J(f(g,h)))_{g=1=h} &= \frac{219}{7}z - \frac{73}{15},\\
S_g\big(Q_2\big(J\big(D_g(D_h(f(g,h)))\big)\big)\big)_{g=1=h} &= \frac{1613}{7}z - \frac{221}{5},\\
S_g^3\big(J\big(D_g^3\big(D_h^3(f(g,h))\big)\big)\big)_{g=1=h} &= \frac{6707861}{4000}z - \frac{10067}{32},\\
J(f(g,h)) &= 8(z+1)g^4 + 16(5z-1)g^5 + 11(6z-2)g^6 + (16z)g^7,\\
S_g(J(f(g,h))) &= \int_0^g \frac{f(J(f(g,h)))}{u}\,\mathrm{d}u\\
&= \int_0^g \frac{8(z+1)u^4 + 16(5z-1)u^5 + 11(6z-2)u^6 + (16z)u^7}{u}\,\mathrm{d}u\\
&= \int_0^g 8(z+1)u^3 + 16(5z-1)u^4 + 11(6z-2)u^5 + (16z)u^6\,\mathrm{d}u\\
&= \left|\frac{8(z+1)u^4}{4} + \frac{16}{5}(5z-1)u^5 + \frac{11}{6}(6z-2)u^6 + \frac{(16z)}{7}u^7\right|_0^g\\
&= \frac{8(z+1)g^4}{4} + \frac{16}{5}(5z-1)g^5 + \frac{11}{6}(6z-2)g^6 + \frac{(16z)}{7}g^7,\\
J\big(D_g(D_h(f(g,h)))\big) &= 32(z+1)g^2 + 96(5z-1)g^3 + 99(6z-2)g^4 + 12(16z)g^5,\\
Q_2\big(J\big(D_g(D_h(f(g,h)))\big)\big) &= Q_2\big[32(z+1)g^2 + 96(5z-1)g^3 + 99(6z-2)g^4 + 12(16z)g^5\big]\\
&= 32(z+1)g^4 + 96(5z-1)g^5 + 99(6z-2)g^6 + 12(16z)g^7,\\
S_g\big(Q_2\big(J\big(D_g(D_h(f(g,h)))\big)\big)\big) &= S_g\begin{bmatrix} 32(z+1)g^4 + 96(5z-1)g^5\\ +99(6z-2)g^6 + 12(16z)g^7 \end{bmatrix}\\
&= \int_0^g \big\{32(z+1)g^4 + 96(5z-1)g^5 + 99(6z-2)g^6 + 12(16z)g^7\big\}\mathrm{d}u\\
&= \left|\frac{32}{4}(z+1)u^4 + \frac{16}{5}(5z-1)u^5 + \frac{11}{6}(6z-2)u^6 + \frac{12}{7}(16z)u^7\right|_0^g\\
&= 8(z+1)g^4 + \frac{96}{5}(5z-1)g^5 + \frac{99}{6}(6z-2)g^6 + \frac{12}{7}(16z)g^7,\\
J\big(D_g^3\big(D_h^3(f(g,h))\big)\big) &= (4)^3 8(z+1)g^2 + (16)^3(16)(5z-1)g^3\\
&\quad + (9)^3(11)(6z-2)g^4 + (12)^3(16z)g^5,\\
S_g^3\big(J\big(D_g^3\big(D_h^3(f(g,h))\big)\big)\big) &= S_g^3\begin{bmatrix} (4)^3 8(z+1)g^2 + (16)^3(16)(5z-1)g^3\\ +(9)^3(11)(6z-2)g^4 + (12)^3(16z)g^5 \end{bmatrix}\\
&= \int_0^g \big|(4)^3 8(z+1)g^2 + (16)^3(16)(5z-1)g^3 + (9)^3(11)(6z-2)g^4 + (12)^3(16z)g^5\big|\mathrm{d}u\\
&= 8\left(\frac{4}{2}\right)^3(z+1)g^2 + 16\left(\frac{6}{3}\right)^3(5z-1)g^3 + \left(\frac{9}{4}\right)^3(11)(6z-2)g^4 + \left(\frac{12}{5}\right)^3(16z)g^5.
\end{aligned}
\tag{33}
$$

Table 7: Comparison among different TIs of (TM-TCNB)[1].

z	$M_1(\mathscr{G}_1)$	$M_2(\mathscr{G}_1)$	$MM_1(\mathscr{G}_1)$	$SDD(\mathscr{G}_1)$
1	658	904	17.7778	249.3333
2	1440	2004	37.1111	540
3	2224	3104	56.4444	830.6667
4	3008	4204	75.7778	1121.3333
5	3792	5304	95.1111	1412
6	4576	6404	114.4444	1702.6667
7	5360	7504	133.7778	1993.3333
8	6144	8604	153.1111	2284
9	6928	9704	172.4444	2574.6667
10	7712	10804	191.7778	2865.3333

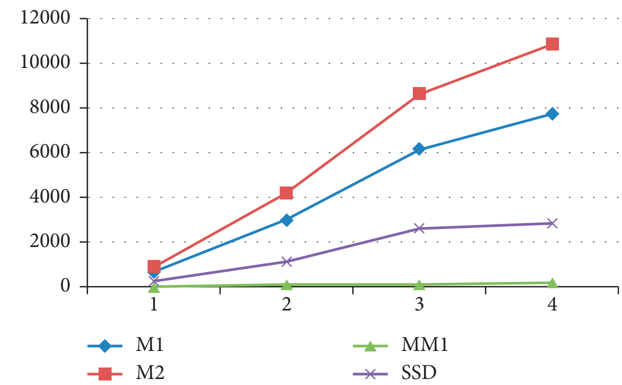

Figure 4: Comparison of computed TIs of (TM-TCNB)[1].

Table 8: Comparison between different TIs of (TM-TCNB)[2].

Z	$M_1(\mathscr{G}_2)$	$M_2(\mathscr{G}_2)$	$MM_1(\mathscr{G}_2)$	$SDD(\mathscr{G}_2)$
1	760	1200	20.8889	292
2	1700	2498	44.8889	646.6667
3	2640	3796	68.8889	1001.3333
4	3580	5094	92.8889	1356.0000
5	4520	6392	116.8889	1710.6667
6	5460	7690	140.8889	2065.3333
7	6400	8988	164.8889	2420.0000
8	7340	10286	188.8889	2774.6667
9	8280	11584	212.8889	3129.3333
10	9220	12882	236.8889	3484

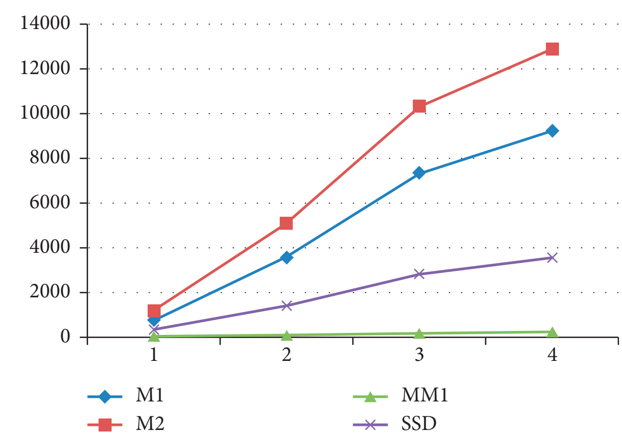

Figure 5: Comparison between different Zagreb indices of (TM-TCNB)[2].

Table 9: Comparison among different TIs of (TM-TCNB)[1].

z	$H(\mathscr{G}_1)$	$IS(\mathscr{G}_1)$	$AZI(\mathscr{G}_1)$
1	45.1048	161.0286	16787.6
2	96.0762	353.6571	37540.2
3	147.0476	546.2857	58292.8
4	198.0190	738.9143	79045.4
5	248.9905	931.5429	99798
6	299.9619	1124.1714	120550.6
7	350.9333	1316.8	141303.2
8	401.9048	1509.4286	162055.8
9	452.8762	1702.0571	182808.4
10	503.8476	1894.6857	203561

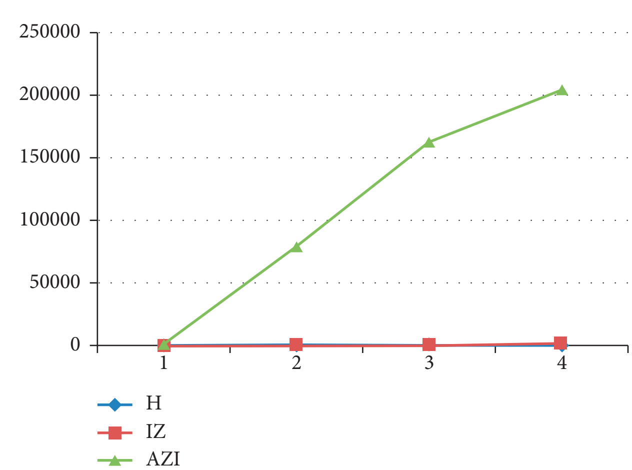

Figure 6: Comparison among different TIs of (TM-TCNB)[1].

Table 10: Comparison among different indices of (TM-TCNB)[2].

z	$H(\mathscr{G}_2)$	$IS(\mathscr{G}_2)$	$AZI(\mathscr{G}_2)$
1	52.8381	186.2286	1362.3715
2	115.4095	416.6571	3039.3367
3	177.9810	647.0857	4716.3020
4	240.5524	877.5143	6393.2672
5	303.1238	1107.9429	8070.2325
6	365.6952	1338.371	9747.1977
7	428.2667	1568.8000	11424.1630
8	490.8381	1799.2286	13101.1282
9	553.4095	2029.6571	14778.0935
10	715.9810	2260.0857	16455.0587

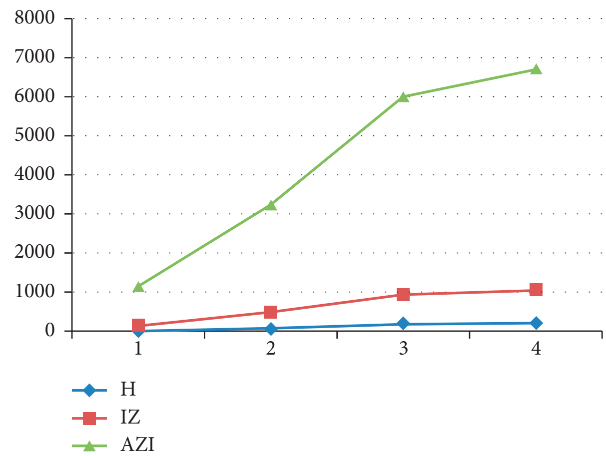

Figure 7: Comparison among different indices of $(\text{TM-TCNB})^2$.

We get

$$
\begin{aligned}
S_g(J(f(g,h)))_{g=1=h} &= \frac{8(z+1)g^4}{4} + \frac{16}{5}(5z-1)g^5 + \frac{11}{6}(6z-2)g^6 + \frac{(16z)}{7}g^7 \\
&= \frac{8(z+1)}{4} + \frac{16}{5}(5z-1) + \frac{11}{6}(6z-2) + \frac{(16z)}{7} = \frac{219}{7}z - \frac{73}{15}, \\
S_g\Big(Q_2\big(J\big(D_g(D_h(f(g,h)))\big)\big)\Big)_{g=1=h} &= 8(z+1)g^4 + \frac{96}{5}(5z-1)g^5 \\
&\quad + \frac{99}{6}(6z-2)g^6 + \frac{12}{7}(16z)g^7 \\
&= 8(z+1) + \frac{96}{5}(5z-1) + \frac{99}{6}(6z-2) + \frac{12}{7}(16z) = \frac{1613}{7}z - \frac{221}{5}, \\
S_g^3\Big(J\big(D_g^3\big(D_h^3(f(g,h))\big)\big)\Big)_{g=1=h} &= 8\left(\frac{4}{2}\right)^3(z+1)g^2 + 16\left(\frac{6}{3}\right)^3(5z-1)g^3 \\
&\quad + \left(\frac{9}{4}\right)^3(11)(6z-2)g^4 + \left(\frac{12}{5}\right)^3(16z)g^5 \\
&= 8\left(\frac{4}{2}\right)^3(z+1) + 16\left(\frac{6}{3}\right)^3(5z-1) + \left(\frac{9}{4}\right)^3(11)(6z-2) + \left(\frac{12}{5}\right)^3(16z) \\
&= \frac{6707861}{4000}z - \frac{10067}{32}.
\end{aligned}
\tag{34}
$$

Now, using Table 2,

$$\begin{aligned} H(\mathscr{G}_2) &= 2S_g(J(f(g,h)))_{g=1=h} \\ &= 2\left\{\frac{219}{7}z - \frac{73}{15}\right\} = \frac{438}{7}z - \frac{146}{15}, \\ IS(\mathscr{G}_2) &= S_g\Big(Q_2\Big(J\Big(D_g\big(D_h(f(g,h))\big)\Big)\Big)\Big)_{g=1=h} \\ &= \frac{1613}{7}z - \frac{221}{5}, \\ AZI(\mathscr{G}_2) &= S_g^3\Big(J\Big(D_g^3\Big(D_h^3(f(g,h))\Big)\Big)\Big)_{g=1=h} \\ &= \frac{6707861}{4000}z - \frac{10067}{32}. \end{aligned} \tag{35}$$

□

4. Comparison and Conclusion

In this section, we calculate various degree-based topological indices and present the results in the form of tables and graphs as given Tables 7–10.

4.1. Comparison between $M_1(\mathscr{G}_1)$ $M_2(\mathscr{G}_1)$, $MM_1(\mathscr{G}_1)$, and $SDD(\mathscr{G}_1)$ of (TM-TCNB)^1. The comparison of first Zagreb $M_1(\mathscr{G}_1)$, second Zagreb $M_2(\mathscr{G}_1)$, second modified Zagreb $MM_1(\mathscr{G}_1)$, and symmetry division deg $SDD(\mathscr{G}_1)$ of (TM-TCNB)^1 is computationally computed with the help of M-polynomials, as given in Table 3. We also computed these indices for different values of z. When z increases, then all TIs are increased in the same order. We show the graphical presentation of all the aforesaid topological indices in Figure 4 for the particular values of z.

4.2. Comparison between $M_1(\mathscr{G}_2)$ $M_2(\mathscr{G}_2)$, $MM_1(\mathscr{G}_2)$, and $SDD(\mathscr{G}_2)$ of (TM-TCNB)^2. The comparison of first Zagreb $M_1(\mathscr{G}_1)$, second Zagreb $M_2(\mathscr{G}_1)$, second modified Zagreb $MM_1(\mathscr{G}_1)$, and symmetry division deg $SDD(\mathscr{G}_1)$ of (TM-TCNB)^2 is computationally computed with the assistance of aforesaid M-polynomials given in Table 4. We calculated these indices for different values of z. When z increases, then all the TIs are increased in the same order. We show the graphical representation of all the degree-based TIs in Figure 5 for the particular values of z.

4.3. Comparison between $H(\mathscr{G}_1)$, $IS(\mathscr{G}_1)$, and $AZI(\mathscr{G}_1)$ of (TM-TCNB)^1. The comparison of the harmonic (H), inverse sum (IS), and augmented Zagreb index (AZI) of (TM-TCNB)^1 is computationally computed with the assistance of M-polynomial given in Table 5. We calculated these indices for different values of z. When z increases, then all the TIs are increased in the same order. We show the graphical representation of all the degree-based TIs in Figure 6 for the particular values of z.

4.4. Comparison between $H(\mathscr{G}_2)$, $IS(\mathscr{G}_2)$, and $AZI(\mathscr{G}_2)$ of (TM-TCNB)^2. The comparison of the harmonic $H(\mathscr{G}_2)$, inverse sum $IS(\mathscr{G}_2)$, and augmented Zagreb index $AZI(\mathscr{G}_2)$ of (TM-TCNB)^2 is computationally computed with the assistance of M-polynomial given in Table 6. We calculated these indices for different values of z. When z increases, then all the TIs are increased in the same order. We show the graphical representation of all the degree-based TIs in Figure 7 for the particular values of z.

In this work, we discussed the M-polynomials of (TM-TCNB)^1 and (TM-TCNB)^2. We also work out on the modern degree-based TIs, including 1st Zagreb (M_1), 2nd Zagreb (M_2), 2nd modified Zagreb (MM_2), general Randic (RR_γ), symmetry division deg (SDD), harmonic (H), inverse sum (IS), and the augmented Zagreb index (AZI) and showed their behavior for (TM-TCNB)^1 and (TM-TCNB)^2. In addition, all the obtained results are also compared with the help of the numerical values provided in the tables, (see Tables 7–10). The problem is still open for the computational results related to different topological indices of the various metal-organic networks.

Data Availability

The data used to support this study are included within the article.

Conflicts of Interest

The authors declare that there are no conflicts of interest.

References

[1] Y. K. Hwang, D.-Y. Hong, J.-S. Chang et al., "Amine grafting on coordinatively unsaturated metal centers of MOFs: consequences for catalysis and metal encapsulation," *Angewandte Chemie International Edition*, vol. 47, no. 22, pp. 4144–4148, 2008.

[2] E. Mohamed, K. Jaheon, R. Nathaniel et al., "Systematic design of pore size and functionality in isoreticular MOFs and their application in methane storage," *Science*, vol. 295, pp. 469–472, 2002.

[3] J. Juan-Alcañiz, J. Gascon, and F. Kapteijn, "Metal-organic frameworks as scaffolds for the encapsulation of active species: state of the art and future perspectives," *Journal of Materials Chemistry*, vol. 22, no. 20, pp. 10102–10118, 2012.

[4] D. Bradshaw, A. Garai, and J. Huo, "Metal-organic framework growth at functional interfaces: thin films and composites for diverse applications," *Chemical Society Reviews*, vol. 41, no. 6, pp. 2344–2381, 2012.

[5] K. Min, F. C. John, F. Honghan, A. P. Kimberley, and M. C. Seth, "Postsynthetic ligand and cation exchange in robust metal-organic frameworks," *Journal of the American Chemical Society*, vol. 134, pp. 18082–18088, 2012.

[6] W. T. Aaron, M. N. Kate, M. H. James, J. H. Anita, and R. H. Matthew, "Metal–Organic frameworks impregnated with magnesium-decorated fullerenes for methane and hydrogen storage," *Journal of the American Chemical Society*, vol. 131, pp. 10662–10669, 2009.

[7] M. Azari and A. Iranmanesh, "Generalized Zagreb index of graphs," *Studia Universitatis Babeş-Bolyai*, vol. 56, no. 3, pp. 59–70, 2011.

[8] K. Won-Tea, Q. Shaopeng, F. O. Alan et al., "Hollow Pd-Ag composite nanowires for fast responding and transparent

hydrogen sensors," *ACS Appl. Matter. Interfaces*, vol. 9, no. 45, pp. 39464–39474, 2017.

[9] R. Seetharaj, P. V. Vandana, P. Arya, and S. Mathew, "Dependence of solvents, pH, molar ratio and temperature in tuning metal organic framework architecture," *Arabian Journal of Chemistry*, vol. 12, no. 3, pp. 295–315, 2019.

[10] L. Hao, W. Kecheng, S. Yujia, T. Christina, L. Jialuo, and Z. Hong-Cai, "Recent advances in gas storage and separation using metal–organic frameworks," *Materials Today*, vol. 21, pp. 221–235, 2018.

[11] H. Y. Min, L. F. Kam, and Z. C. George, "Study suggests choice between green energy or economic growth," *Green Energy and Environment*, vol. 2, pp. 218–245, 2017.

[12] L. R. Biao, X. Shengchang, X. Huabin, Z. Wei, and C. Banglin, "Exploration of porous metal–organic frameworks for gas separation and purification," *Coordination Chemistry Reviews*, vol. 378, pp. 87–103, 2019.

[13] V. Alexander, "Upper and lower bounds of symmetric division deg index," *Iran J Math Chem*, vol. 52, pp. 91–108, 2014.

[14] C. W. Megan, L. Jiafei, I. Timur, and K. F. Omar, "Linker competition within a metal-organic framework for topological insights," *American Chemical Society*, vol. 58, no. 2, pp. 1513–1517, 2019.

[15] C. Petit and T. J. Bandosz, "MOF-graphite oxide composites: combining the uniqueness of graphene layers and metal-organic frameworks," *Advanced Materials*, vol. 21, no. 46, pp. 4753–4757, 2009.

[16] J. Y. Seung, Y. C. Jae, K. C. Hee, H. C. Jung, S. N. Kee, and R. P. Chong, "Preparation and enhanced hydrostability and hydrogen storage capacity of CNT@MOF-5 hybrid composite," *Chemistry of Materials*, vol. 21, pp. 1893–1897, 2009.

[17] G. Rücker and C. Rücker, "On topological indices, boiling points, and cycloalkanes," *Journal of Chemical Information and Computer Sciences*, vol. 39, no. 5, pp. 788–802, 1999.

[18] F. M. Bruckler, T. Doslic, A. Graovac, and I. Gutman, "On a class of distance-based molecular structure descriptors," *Chemical Physics Letters*, vol. 503, pp. 336–338, 2011.

[19] H. Gonzalez-Diaz, S. Vilar, L. Santana, and E. Uriarte, "Medicinal chemistry and bioinformatics-current trends in drugs discovery with networks topological indices," *Current Topics in Medicinal Chemistry*, vol. 7, no. 10, pp. 1015–1029, 2007.

[20] S. Klavzar and I. Gutman, "A comparison of the Schultz molecular topological index with the wiener index," *Journal of Chemical Information and Computer Sciences*, vol. 36, pp. 1001–1003, 1996.

[21] A. R. Matamala and E. Estrada, "Generalised topological indices: optimisation methodology and physico-chemical interpretation," *Chemical Physics Letters*, vol. 410, no. 4-6, pp. 343–347, 2005.

[22] M. Randic, "Characterization of molecular branching," *Journal of the American Chemical Society*, vol. 97, no. 23, pp. 6609–6615, 1975.

[23] B. Furtula and I. Gutman, "A forgotten topological index," *Journal of Mathematical Chemistry*, vol. 53, no. 4, pp. 1184–1190, 2015.

[24] X. Li and J. Zheng, "Extremal chemical trees with minimum or maximum general Randic index," *MATCH Communications in Mathematical and in Computer Chemistry*, vol. 54, pp. 195–205, 2005.

[25] A. M. Naji, N. D. Soner, and I. Gutman, "On leap Zagreb indices of graphs," *Communications in Combinatorics and Optimization*, vol. 2, pp. 99–117, 2017.

[26] H. Wiener, "Structural determination of paraffin boiling points," *Journal of the American Chemical Society*, vol. 69, no. 1, pp. 17–20, 1947.

[27] I. Gutman and N. Trinajstić, "Graph theory and molecular orbitals. Total φ-electron energy of alternant hydrocarbons," *Chemical Physics Letters*, vol. 17, no. 4, pp. 535–538, 1972.

[28] I. Gutman and O. Polansky, *Mathematical Concepts in Organic Chemistry*, Springer-Verlag, New York, NY, USA, 1986.

[29] J. Devillers, D. Domine, C. Guillon, S. Bintein, and W. Karcher, "Prediction of partition coefficients (LOGPoct) using autocorrelation descriptors," *SAR and QSAR in Environmental Research*, vol. 7, no. 1-4, pp. 151–172, 1997.

[30] B. Rajan, A. William, C. Grigorious, and S. Stephen, "On certain topological indices of silicate, honeycomb and hexagonal networks," *Journal of Mathematical and Computational Science*, vol. 3, no. 5, pp. 530–535, 2012.

[31] M. Javaid, M. A. Ur Rehman, and J. Cao, "Topological indices of rhombus type silicate and oxide networks," *Canadian Journal of Chemistry*, vol. 95, pp. 134–143, 2016.

[32] M. Javaid, J.-B. Liu, M. A. Rehman, and S. Wang, "On the certain topological indices of titania nanotube $TiO_2[m, n]$," *Zeitschrift für Naturforschung A*, vol. 72, no. 7, pp. 647–654, 2017.

[33] X. Guiyin, N. Ping, D. Hui, D. Bing, L. Laiyang, and Z. Xiaogang, "Harvard enters superconducting spin cycle," *Materials Today*, vol. 20, pp. 22–35, 2017.

[34] W. Hailong, Z. Qi-Long, Z. Ruqiang, and X. Qiang, "Metal-organic frameworks for energy applications," *Chememistry*, vol. 2, pp. 52–80, 2017.

[35] S. Akhter and M. Imran, "On molecular topological properties of benzenoid structures," *Canadian Journal of Chemistry*, vol. 94, no. 8, pp. 687–698, 2016.

[36] J. Baca, M. Horvathova, M. Mokrisova, and A. Suhanyiova, "On topological indices of fullerenes," *Applied Mathematics and Computation*, vol. 251, pp. 154–161, 2015.

[37] M. Baca, J. Horvathova, M. Mokrisova, A. Suhanyiova, and S.-F. Andrea, "On topological indices of carbon nanotube network," *Canadian Journal of Chemistry*, vol. 93, pp. 1157–1160, 2015.

[38] S. Wang and S. Ji, "On the sharp lower bounds of Zagreb indices of graphs with given number of cut vertices," *Journal of Mathematical Analysis and Applications*, vol. 458, no. 1, pp. 21–29, 2018.

[39] S. Wang, C. Wang, L. Chen, and J.-B. Liu, "On extremal multiplicative Zagreb indices of trees with given number of vertices of maximum degree," *Discrete Applied Mathematics*, vol. 227, pp. 166–173, 2017.

[40] P. S. Ranjini, V. Lokesha, and A. Usha, "On the symmetric division deg index of graph," *The International Journal of Graph Theory*, vol. 1, pp. 116–121, 2013.

[41] A. Kashif, S. Aftab, M. Javaid, and H. M. Awais, "M-polynomial-based topological indices of metal-organic networks," *Main Group Metal Chemistry*, vol. 44, no. 1, pp. 129–140, 2021.